SCIENCE CHINA
Chemistry

•COMMUNICATIONS•
SPECIAL TOPIC: Photocatalytic or Electrocatalytic Reduction of CO_2

December 2020 Vol.63 No.12: 1711–1715
https://doi.org/10.1007/s11426-020-9825-9

CO_2 electrolysis at industrial current densities using anion exchange membrane based electrolyzers

Pengfei Wei[1,2], Hefei Li[1,2], Long Lin[1,2], Dunfeng Gao[1*], Xiaomin Zhang[1], Huimin Gong[1], Guangyan Qing[1], Rui Cai[1], Guoxiong Wang[1*] & Xinhe Bao[1]

[1]*State Key Laboratory of Catalysis, Dalian National Laboratory for Clean Energy, Dalian Institute of Chemical Physics, Chinese Academy of Sciences, Dalian 116023, China;*
[2]*University of Chinese Academy of Sciences, Beijing 100049, China*

Received June 19, 2020; accepted July 11, 2020; published online August 25, 2020

Significant progress on electrocatalytic CO_2 reduction reaction (CO_2RR) has been achieved in recent years. However, the research and development of electrolyzer device for CO_2RR is scarce. Here we use anion exchange membrane to develop zero-gap electrolyzers for CO_2RR. The electrochemical properties of the electrolyzers with Pd/C and Cu cathodes are investigated. The Pd/C cathode shows a current density of 200 mA cm^{-2} with CO Faradaic efficiency of 98% and energy efficiency of 48.8%, while the Cu cathode shows a current density of 350 mA cm^{-2} with total CO_2RR Faradaic efficiency of 81.9% and energy efficiency of 30.5%. This work provides a promising demonstration of CO_2 electrolyzer using anion exchange membrane for CO_2 electrolysis at industrial current densities.

CO_2 electrolysis, electrolyzer, industrial current density, anion exchange membrane, energy efficiency, Pd/C catalyst, Cu catalyst

Citation: Wei P, Li H, Lin L, Gao D, Zhang X, Gong H, Qing G, Cai R, Wang G, Bao X. CO_2 electrolysis at industrial current densities using anion exchange membrane based electrolyzers. *Sci China Chem*, 2020, 63: 1711–1715, https://doi.org/10.1007/s11426-020-9825-9

Electrocatalytic CO_2 reduction reaction (CO_2RR) that converts CO_2 and H_2O to useful chemicals and feedstock is a promising route to address the conversion and utilization of CO_2 as well as the storage of renewable energy simultaneously [1]. In recent years, many efforts have been devoted to designing efficient catalysts in order to reduce the overpotential and improve the Faradaic efficiency and current density of CO_2RR. Significant progress has been achieved for catalyzing CO_2RR to CO, formate, ethylene, ethanol and other hydrocarbons/oxygenates [2–11]. However, most electrochemical results are usually acquired in H-type cells, and the current density of CO_2RR is limited by low solubility of CO_2 in aqueous solutions and only reaches a few tens of mA cm^{-2} [12]. Flow cells can improve the current density of CO_2RR up to a few hundred of mA cm^{-2} even A cm^{-2} by constructing the three-phase boundary of CO_2 gas/liquid electrolyte/solid catalyst in gas diffusion electrode configuration, however, the liquid electrolyte between cathode and anode causes a huge voltage drop and a low energy efficiency due to a large ohmic loss [13]. The most practical way is to develop zero-gap CO_2 electrolyzers using solid polymer electrolyte membranes [14–20]. As the membrane is very thin (usually tens of μm) and has very good ion conductivity, the ohmic loss can be drastically decreased for meeting the industrial requirements of high current density and energy efficiency. Since hydrogen evolution reaction (HER) can be efficiently suppressed in alkaline environments, anion exchange membrane (AEM) is preferred in zero-gap CO_2 electrolyzers. However, to date only a few literatures reported CO_2RR performances in AEM-based electrolyzers

*Corresponding authors (email: dfgao@dicp.ac.cn; wanggx@dicp.ac.cn)

[3–6,21–25] and the electrochemical properties of these AEM-based electrolyzers are not well understood.

In this work, AEM-based CO_2 electrolyzer was constructed using Pd/C and Cu catalysts as cathode catalysts, which are dominant for CO and hydrocarbon/oxygenate production, respectively. The electrochemical properties of the AEM-based CO_2 electrolyzer was investigated under different reaction conditions. The cell voltage was obviously decreased while the total Faradaic efficiency of CO_2RR products increased slightly when an alkaline aqueous solution was fed into the anode. The use of polytetrafluoroethylene (PTFE) instead of Nafion ionomer as the binder in cathode catalyst layer improved the CO Faradaic efficiency over Pd/C cathode and hydrocarbon/oxygenate Faradaic efficiency over Cu cathode at high current densities, thus enhancing the energy efficiency of the CO_2 electrolyzer.

The Pd/C catalyst was synthesized with a wet chemical reduction method as reported previously by our group [12]. Figure 1(a) shows the transmission electron microscopy (TEM) images of the Pd/C catalyst where the Pd nanoparticles (NPs) are dispersed homogeneously on carbon support. The metallic state in the bulk of Pd NPs is confirmed by the typical X-ray diffraction (XRD) patterns in Figure S1 (a) (Supporting Information online). The other cathode catalyst used in this work is commercial Cu NPs. As shown in

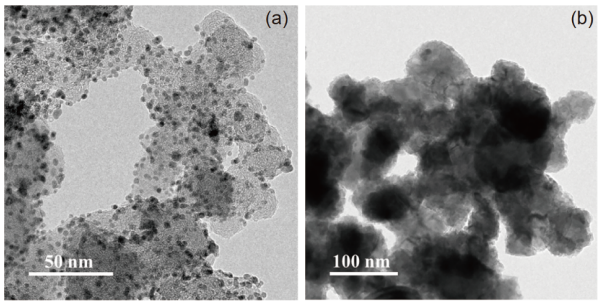

Figure 1 TEM images of Pd/C (a) and Cu (b) catalysts.

Figure 1(b), Cu NPs tend to form aggregates with size distributions from tens of nm to more than one hundred nm. However, the crystalline size of Cu NPs is around 25 nm as calculated from the Cu (111) peak of XRD patterns in Figure S1(b). The presence of strong Cu_2O peaks also indicates that the commercial Cu NPs are severely oxidized, which however does not affect the CO_2RR performance due to the *in situ* reduction of Cu oxides under reaction conditions [6].

Figure 2 shows the configuration of an AEM-based CO_2 electrolyzer. One graphite flow field plate and one Au-coated stainless steel plate were used for CO_2 feeding and current collecting at the cathode, respectively, while one titanium flow field plate was used for aqueous solution feeding and

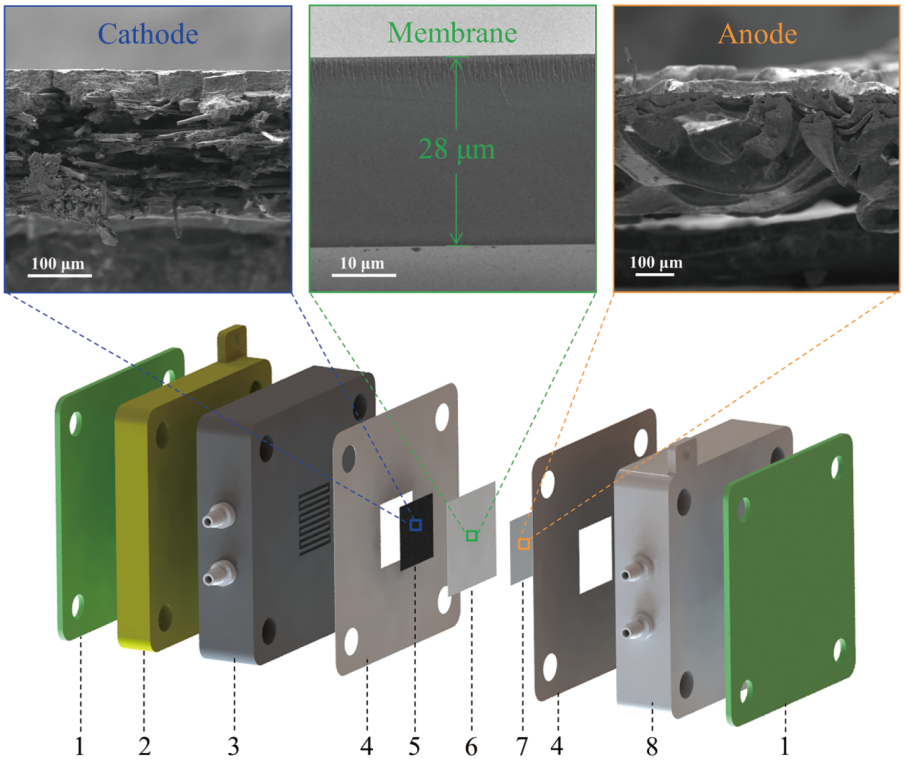

Figure 2 Schematic of AEM-based CO_2 electrolyzer and cross-sectional SEM images of Pd/C cathode, QAPPT anion exchange membrane and IrO_2-coated Ni foam anode (color online).

current collecting at the anode. The catalyst-coated (Pd/C or Cu NPs) carbon paper and IrO_2-coated Ni foam were used as the cathode and anode, respectively, while the quaternary ammonia poly(*N*-methyl-piperidine-*co*-*p*-terphenyl) (QAPPT) membrane was used as the anion electrolyte membrane. The cathode, membrane and anode constitutes membrane assembly electrode (MEA) that is the core of an AEM-based CO_2 electrolyzer [5,14,20]. Figure 2 also shows the cross-sectional scanning electron microscopy (SEM) images of the Pd/C cathode, QAPPT membrane and IrO_2-coated Ni foam anode. The QAPPT membrane has a thickness of 28 μm. The morphology and energy-dispersive X-ray spectroscopy (EDS) elemental maps of the Pd/C and Cu cathodes as well as the IrO_2-coated Ni foam anode are shown in Figures S2–S6.

With the AEM-based CO_2 electrolyzer, we measured the CO_2 electrolysis performance of the Pd/C and Cu cathodes under industrial current densities. The cathode is fed with the CO_2 gas, while the anode is fed with 0.1 M $KHCO_3$ and 0.1 M KOH aqueous solutions, respectively. Figure 3 shows Faradaic efficiencies of various products and cell voltages as a function of applied current densities. CO is the major product over the Pd/C cathode at the current density from 50 to 200 mA cm^{-2} with CO Faradaic efficiency of >95% in both cases of 0.1 M $KHCO_3$ and 0.1 M KOH (Figure 3(a, b)). However, the CO Faradaic efficiency sharply drops to 58.7% at 250 mA cm^{-2} and 32.7% at 300 mA cm^{-2} in the case of 0.1 M $KHCO_3$. It is worth noting that the decrease in CO Faradaic efficiency is less significant in the case of 0.1 M KOH, with 87.2% at 250 mA cm^{-2} and 55.0% at 300 mA cm^{-2}. Over the Cu cathode, multicarbon (C_{2+}) hydrocarbons and oxygenates such as ethylene, ethanol and acetic acid, were produced besides CO and H_2. The Faradaic efficiencies of C_{2+} products increase while CO Faradaic efficiency decreases with the current density of up to 250 mA cm^{-2} in the case of 0.1 M $KHCO_3$, suggesting that CO is a key reaction intermediate for C_{2+} production [2,6,18]. When the cathode is fed with 0.1 M KOH aqueous solution, the changes in the voltage-dependent Faradaic efficiencies of CO and C_{2+} follow similar trends while Faradaic efficiencies of C_{2+} and C_2H_4 become slightly higher (Figure 3 (c, d)). The maximum C_{2+} and C_2H_4 Faradaic efficiencies are 64.2% and 32.5% at 300 mA cm^{-2} in the case of 0.1 M KOH. The cell voltages of both Pd/C and Cu cathodes are lower in the case of 0.1 M KOH compared to 0.1 M $KHCO_3$. The difference in the cell voltage is attributed to the reduction of thermodynamic voltage of full reaction due to the OH^- concentration gradient in the presence of KOH [20]. On the other hand, the increased pH due to the diffusion of KOH through membrane is favorable to suppress HER at high current densities [4,10]. Nevertheless, here we are able to improve CO_2RR Faradaic efficiency and decrease cell voltage at high current densities by feeding 0.1 M KOH instead of 0.1 M $KHCO_3$ at the anode.

The obviously increased H_2 Faradaic efficiency over the Pd/C and Cu cathodes at high current densities may be ascribed to two possible reasons. One is that the kinetics of facile HER increases more quickly than that of sluggish

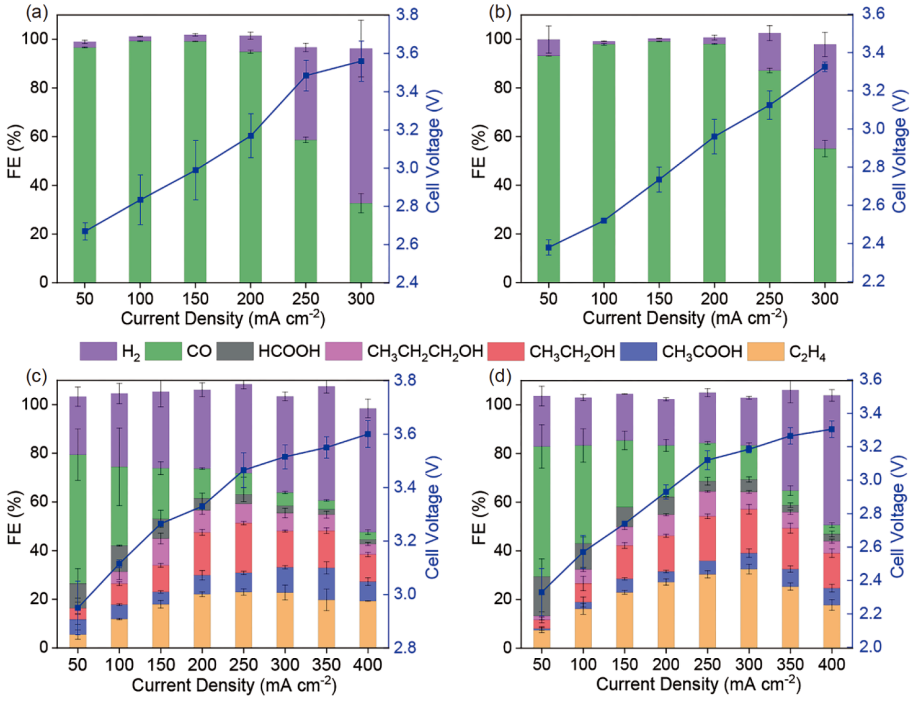

Figure 3 Faradaic efficiency (FE) and current density-voltage curves of the Pd/C (a, b) and Cu (c, d) cathodes measured in 0.1 M $KHCO_3$ (a, c) and 0.1 M KOH (b, d) with Nafion as a binder (color online).

CO_2RR with increasing overpotentials. The other one is that CO_2 mass transport is limited by the excess water at the cathode [26]. In order to improve the CO_2 mass transport of cathode, PTFE was used as the binder to replace Nafion ionomer in cathode catalyst layer. Figure 4(a) and Figure S7 (a) show that the PTFE-bounded Pd/C cathode improves CO Faradaic efficiency at current densities of >200 mA cm^{-2} compared to the Nafion-bounded Pd/C cathode. The PTFE-bonded Cu cathode shows an improved Faradaic efficiency and current density of CO_2RR than the Nafion-bounded Cu cathode (Figure 4(b) and Figure S7(b)). Therefore, the CO_2 electrolysis performance of AEM-based electrolyzers could be significantly improved by enhancing the mass transport of CO_2 at the cathode. Energy efficiencies were calculated based on applied cell voltages and thermoneutral voltages (Table S1, Supporting Information online) in combination with Faradaic efficiencies of desired CO_2RR products (See Supporting Information online for calculation details). Figure 4(c, d) show energy efficiencies of the Pd/C and Cu cathodes with PTFE and Nafion as a binder in cathode catalyst layer. The Pd/C cathode with the Nafion binder shows a current density of 200 mA cm^{-2} with CO Faradaic efficiency of 98% and energy efficiency of 48.8%, while the Cu cathode with the PTFE binder shows a current density of 350 mA cm^{-2} with total CO_2RR Faradaic efficiency of 81.9% and energy efficiency of 30.5%. The role of the PTFE binder is minor at low current densities but becomes significant at high current densities. For instance, the energy efficiency of the Pd/C cathode for CO production increases from 6.3% in the case of Nafion to 28.6% in the case of PTFE at 350 mA cm^{-2} and it increases from 10.7% to 21.3% over the Cu cathode for C_{2+} production at 450 mA cm^{-2}. In comparison with previously reported AEM electrolyzers [4–6,16,21–24], our electrolyzer shows very promising CO_2 electrolysis performance in terms of current density, Faradaic efficiency as well as energy efficiency (Table S2).

Under the optimized conditions with 0.1 M KOH electrolyte and PTFE binder, we performed stability tests over the Pd/C and Cu cathodes in the AEM-based electrolyzer (Figures S8 and S9). The stability test of the Pd/C cathode was conducted at a constant current density of 100 mA cm^{-2}. As shown in Figure S8, the CO Faradaic efficiency keeps almost unchanged at around 98% and the cell voltage increases from 2.6 to 2.8 V during the measurement of 40 h. At the constant current density of 200 mA cm^{-2}, the Cu cathode shows stable C_2H_4 Faradaic efficiency of 30% and cell voltage of 2.85 V in the course of 22 h, respectively (Figure S9). These results indicate that our AEM-based electrolyzer delivers a stable performance for continuous production of CO and hydrocarbons at industrial current densities.

In summary, an AEM-based electrolyzer device was developed to evaluate CO_2 electrolysis performance at industrial current densities. The Pd/C and Cu cathodes show high Faradaic efficiency for CO and multicarbon hydrocarbon/oxygenate production, respectively. The alkaline electrolyte at the anode is beneficial to decrease cell voltage

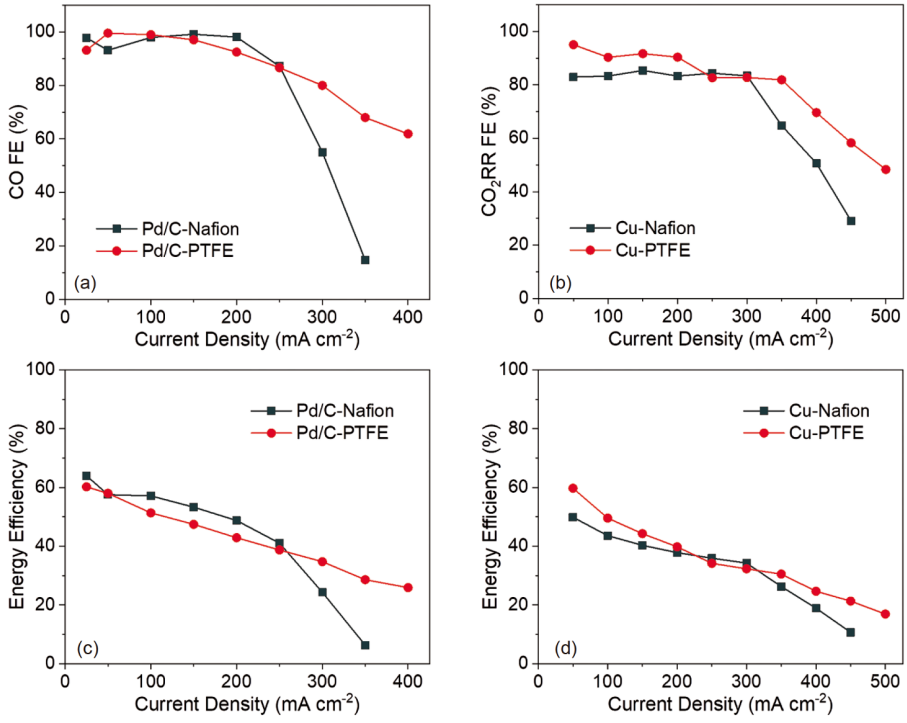

Figure 4 CO Faradaic efficiency (a) and energy efficiency (c) of the Pd/C cathode as well as total CO_2RR Faradaic efficiency (b) and energy efficiency (d) of the Cu cathode measured in 0.1 M KOH with Nafion or PTFE as a binder (color online).

and suppress HER at the cathode. Improving the mass transport of CO_2 in cathode catalyst layer is critical to improve the Faradaic efficiency and current density of CO_2 electrolysis at high current densities. Under optimized reaction conditions, the Pd/C cathode shows a current density of 200 mA cm^{-2} with CO Faradaic efficiency of 98% and energy efficiency of 48.8%, while the Cu cathode shows a current density of 350 mA cm^{-2} with total CO_2RR Faradaic efficiency of 81.9% and energy efficiency of 30.5%. The AEM-based electrolyzer presented in this work holds promise for practical electrocatalytic CO_2 conversion to fuels and chemicals.

Although current density, Faradaic efficiency and energy efficiency of current CO_2 electrolyzers for CO production are almost at the industry level (Table S2), to date only quite few studies have demonstrated CO_2 electrolysis at an industrially relevant time scale of thousands of hours [16,27]. Current issues regarding to the long-term performance and stability [1], another key parameter for practical application, should be well addressed in the future. In the case of CO_2RR to higher-value C_{2+} products such as ethylene and ethanol, selectivity towards single specific product at industrial current densities should be further improved so as to reduce the cost of downstream separation and purification.

Acknowledgements This work was supported by the National Key R&D Program of China (2016YFB0600901), the National Natural Science Foundation of China (21573222, 91545202), Dalian National Laboratory for Clean Energy (DNL180404, DNL201924), Dalian Institute of Chemical Physics (DMTO201702), Dalian Outstanding Young Scientist Foundation (2017RJ03), the Strategic Priority Research Program of the Chinese Academy of Sciences (XDB17020200), and the CAS Youth Innovation Promotion (Y201938).

Conflict of interest The authors declare no conflict of interest.

Supporting information The supporting information is available online at http://chem.scichina.com and http://link.springer.com/journal/11426. The supporting materials are published as submitted, without typesetting or editing. The responsibility for scientific accuracy and content remains entirely with the authors.

1 Chen C, Khosrowabadi Kotyk JF, Sheehan SW. *Chem*, 2018, 4: 2571–2586
2 Gao D, Arán-Ais RM, Jeon HS, Roldan Cuenya B. *Nat Catal*, 2019, 2: 198–210
3 Li F, Thevenon A, Rosas-Hernández A, Wang Z, Li Y, Gabardo CM, Ozden A, Dinh CT, Li J, Wang Y, Edwards JP, Xu Y, McCallum C, Tao L, Liang ZQ, Luo M, Wang X, Li H, O'Brien CP, Tan CS, Nam DH, Quintero-Bermudez R, Zhuang TT, Li YC, Han Z, Britt RD, Sinton D, Agapie T, Peters JC, Sargent EH. *Nature*, 2020, 577: 509–513
4 Ren S, Joulié D, Salvatore D, Torbensen K, Wang M, Robert M, Berlinguette CP. *Science*, 2019, 365: 367–369
5 Yin Z, Peng H, Wei X, Zhou H, Gong J, Huai M, Xiao L, Wang G, Lu J, Zhuang L. *Energy Environ Sci*, 2019, 12: 2455–2462
6 Gabardo CM, O'Brien CP, Edwards JP, McCallum C, Xu Y, Dinh CT, Li J, Sargent EH, Sinton D. *Joule*, 2019, 3: 2777–2791
7 Zhu W, Kattel S, Jiao F, Chen JG. *Adv Energy Mater*, 2019, 9: 1802840
8 Shao J, Wang Y, Gao D, Ye K, Wang Q, Wang G. *Chin J Catal*, 2020, 41: 1393–1400
9 Li S, Saranya G, Chen M, Zhu Y. *Sci China Chem*, 2020, 63: 722–730
10 Ye K, Cao A, Shao J, Wang G, Si R, Ta N, Xiao J, Wang G. *Sci Bull*, 2020, 65: 711–719
11 Jia S, Zhu Q, Wu H, Chu M, Han S, Feng R, Tu J, Zhai J, Han B. *Chin J Catal*, 2020, 41: 1091–1098
12 Gao D, Zhou H, Wang J, Miao S, Yang F, Wang G, Wang J, Bao X. *J Am Chem Soc*, 2015, 137: 4288–4291
13 Salvatore D, Berlinguette CP. *ACS Energy Lett*, 2020, 5: 215–220
14 Weekes DM, Salvatore DA, Reyes A, Huang A, Berlinguette CP. *Acc Chem Res*, 2018, 51: 910–918
15 Gao D, Cai F, Xu Q, Wang G, Pan X, Bao X. *J Energy Chem*, 2014, 23: 694–700
16 Kutz RB, Chen Q, Yang H, Sajjad SD, Liu Z, Masel IR. *Energy Technol*, 2017, 5: 929–936
17 Salvatore DA, Weekes DM, He J, Dettelbach KE, Li YC, Mallouk TE, Berlinguette CP. *ACS Energy Lett*, 2018, 3: 149–154
18 Gutiérrez-Guerra N, González JA, Serrano-Ruiz JC, López-Fernández E, Valverde JL, de Lucas-Consuegra A. *J Energy Chem*, 2019, 31: 46–53
19 Wang G, Pan J, Jiang SP, Yang H. *J CO_2 Utilization*, 2018, 23: 152–158
20 Weng LC, Bell AT, Weber AZ. *Energy Environ Sci*, 2019, 12: 1950–1968
21 Reyes A, Jansonius RP, Mowbray BAW, Cao Y, Wheeler DG, Chau J, Dvorak DJ, Berlinguette CP. *ACS Energy Lett*, 2020, 5: 1612–1618
22 Larrazábal GO, Strøm-Hansen P, Heli JP, Zeiter K, Therkildsen KT, Chorkendorff I, Seger B. *ACS Appl Mater Interfaces*, 2019, 11: 41281–41288
23 Lee WH, Ko YJ, Choi Y, Lee SY, Choi CH, Hwang YJ, Min BK, Strasser P, Oh HS. *Nano Energy*, 2020, 76: 105030
24 Ma C, Hou P, Wang X, Wang Z, Li W, Kang P. *Appl Catal B-Environ*, 2019, 250: 347–354
25 Lee J, Lim J, Roh CW, Whang HS, Lee H. *J CO_2 Utilization*, 2019, 31: 244–250
26 Wakerley D, Lamaison S, Ozanam F, Menguy N, Mercier D, Marcus P, Fontecave M, Mougel V. *Nat Mater*, 2019, 18: 1222–1227
27 Haas T, Krause R, Weber R, Demler M, Schmid G. *Nat Catal*, 2018, 1: 32–39